

# A Fault Tolerant Control strategy for an Unmanned Aerial Vehicle based on a Sequential Quadratic Programming Algorithm

François Bateman, Hassan Noura and Mustapha Ouladsine

**Abstract**—In this paper a Fault Tolerant Control strategy for the nonlinear model of an unmanned aerial vehicle (UAV) equipped with numerous redundant controls is proposed. Asymmetric actuator failures are considered and, in order to accommodate them, a Sequential Quadratic Programming (SQP) algorithm which takes into account nonlinearities, aerodynamic and gyroscopic couplings, state and control limitations is implemented. This algorithm computes new trims such that around the new operating point, the faulty linearized model remains nearby from the fault free model. For the faulty linearized models, linear state feedback controllers based on an eigenstructure assignment method are designed to obtain soft transients during accommodation. Real time implementation of the SQP algorithm is also discussed.

## I. INTRODUCTION

Poor reliability record, absence of certification standards and regulations addressing UAV systems slows down their integration in the civil airspaces. The future UAV standard USAR [4] suggests a mishap rate of one catastrophic mishap per  $1.10^6$  flying hours. A recent study [7] showed that Flight Control Systems (FCS) were involved in numerous incidents, these systems includes all systems contributing to the aircraft stability and control such as avionics, air data system, servo-actuators, control surfaces/servos, on-board software, navigation, and other related subsystems. As regards FCS, failures are often critical [5], they may originate from icing, hydraulic failure, combat damages. To overcome UAV reliability, [6] recommends to adopt a better component selection methodology, the use of advanced digital avionics systems and self-repairing, smart FCS.

Fault tolerant control (FTC) strategies applied to control surface failures has received considerable attention. However, little research has been carried out on asymmetric failures. For these faults, coupling appear between axis and may break the equilibrium of forces and moments. On the other hand, time required to process the failure may move the state vector far away from its operating point. For these reasons a nonlinear model of the aircraft taking into account aerodynamical effects of each control surface must be considered.

With regards to asymmetric control surfaces failures, a passive accommodation strategy based on a dynamic inversion control law was proposed in [9] for a reentry vehicle. Fault tolerant Control (FTC) strategies using

neural networks with on-line learning were presented in [12], [13]. Thomas [15] implements a nonlinear controller and processes the nonlinear model of the aircraft with a numerical model. As regards active accommodation, it is worth to notice that the formalisms used in these papers make difficult physical interpretations. Recently, a multiple model approach taking into account model limitations was developed in [10], this method allows conciliating model complexity and physical interpretations in the sense of flying mechanics.

Moreover, in the case of control surface failures, an effective re-allocation of the remaining healthy control actuators is needed in order to achieve acceptable performances. Two reconfiguration strategies for nonlinear affine in control systems are proposed in [8], the first one uses optimal control to decide the control input directly, and the second using optimal control to decide the total control effort and then using control allocation to compute the control input. The methods are illustrated with a jetfighter FCS. Zhang [16] implements a cascaded generalized algorithm (CGI) for a jetfighter. When an actuator is saturated this algorithm deals with control saturations by redistributing the remaining controls to achieve the desired moment.

The FTC method proposed in this paper deals with accommodation for the nonlinear model of a UAV, moreover it takes into account control saturations. On the other hand, as it is based on the complete analytical model of the aircraft, it allows giving physical interpretations. In this way, control laws for the accommodation are designed by considering handling qualities problem. The paper is organized as follows, in section II a nonlinear model of the UAV including eight independent actuators is described. In section III, control surfaces failures are considered and a fault tolerant method mixed with a Sequential Programming Quadratic (SQP) algorithm associated with a state feedback controller using eigenstructure assignment method is described. Moreover, some considerations about SQP real time implementation are given. Results and perspectives are given in section IV and V.

## II. THE UAV MODEL

The UAV studied and shown on figure 1 is a real single-engined with high wing. It is provided with seven control surfaces and a throttle. In the presence of ac-

tuator failures, the healthy controls provide redundancies which allow maintaining the aircraft in flight. It is assumed that the aircraft is rigid-body, weight  $m$  is constant and centre of gravity  $c.g.$  is fixed position. Its state vector is  $X = (\varphi \ \theta \ V \ \alpha \ \beta \ p \ q \ r)^T$  where  $\varphi$  is the bank angle,  $\theta$  the pitch angle,  $V$  the true airspeed,  $\alpha$  the angle of attack,  $\beta$  the sideslip,  $p$  the roll,  $q$  the pitch, and  $r$  the yaw. The control vector  $U = (\delta_x \ \delta_{ar} \ \delta_{al} \ \delta_{fr} \ \delta_{fl} \ \delta_{er} \ \delta_{el} \ \delta_r)^T$  where  $\delta_x$  is the throttle,  $\delta_{ar}$  and  $\delta_{al}$  are the right and left ailerons,  $\delta_{fr}$  and  $\delta_{fl}$  are the right and left flaps,  $\delta_{er}$  and  $\delta_{el}$  are the right and left elevators and  $\delta_r$  is the rudder. All the state variables are measured.

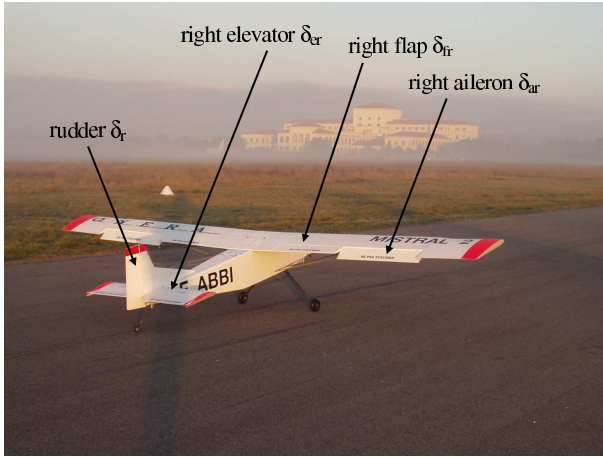


Fig. 1. The UAV and its control surfaces

Angles  $\varphi$ ,  $\theta$  and  $\psi$  locate the body-fixed reference frame  $R_b$  in the earth-fixed reference frame  $R_E$ , the transformation from  $R_b$  to  $R_E$  is expressed by the transformation matrix  $\mathbf{T}_{be}$ :

$$\begin{pmatrix} \cos\theta\cos\psi & \sin\varphi\sin\theta\cos\psi - \cos\varphi\sin\psi & \cos\varphi\sin\theta\cos\psi + \sin\varphi\sin\psi \\ \cos\theta\sin\psi & \sin\varphi\sin\theta\sin\psi + \cos\varphi\cos\psi & \cos\varphi\sin\theta\sin\psi - \sin\varphi\cos\psi \\ -\sin\theta & \sin\varphi\cos\theta & \cos\varphi\cos\theta \end{pmatrix} \quad (1)$$

Angles  $\alpha$  and  $\beta$  locate the aerodynamic reference frame  $R_a$  in  $R_b$ , the transformation from  $R_b$  to  $R_a$  is expressed by the transformation matrix  $\mathbf{T}_{ba}$ :

$$\begin{pmatrix} \cos\alpha\cos\beta & \sin\beta & \sin\alpha\cos\beta \\ -\cos\alpha\sin\beta & \cos\beta & -\sin\alpha\sin\beta \\ -\sin\alpha & 0 & \cos\alpha \end{pmatrix} \quad (2)$$

In the body-fixed reference frame  $R_b$ , the linear velocity  $\vec{V}_{c.g.}^{[R_b]} = (u \ v \ w)^T$  and the angular velocity  $\vec{\Omega}_{R_b/R_E}^{[R_b]} = (p \ q \ r)^T$  derive from the general force  $\vec{F}$  equation and from the general moment  $\vec{\Gamma}_{c.g.}$  measured around  $c.g.$ :

$$\vec{F} = m \left( \frac{d\vec{V}_{c.g.}^{[R_b]}}{dt} + \vec{\Omega}_{R_b/R_E}^{[R_b]} \wedge \vec{V}_{c.g.}^{[R_b]} \right) \quad (3)$$

$$\vec{\Gamma}_{c.g.} = I \frac{d\vec{\Omega}^{[R_b]}}{dt} + \vec{\Omega}_{R_b/R_E}^{[R_b]} \wedge I \vec{\Omega}^{[R_b]} \quad (4)$$

where the inertia matrix is defined as:

$$\mathbf{I} = \begin{pmatrix} I_{xx} & 0 & -I_{xz} \\ 0 & I_{yy} & 0 \\ -I_{zx} & 0 & I_{zz} \end{pmatrix} \quad (5)$$

The true airspeed  $V$ , the angle of attack  $\alpha$  and the sideslip  $\beta$  are expressed with the body-axis velocities  $u$ ,  $v$ ,  $w$  and the transformation matrix  $T_{ba}$ , [3]:

$$V = \sqrt{u^2 + v^2 + w^2} \quad (6)$$

$$\alpha = \arctan\left(\frac{w}{u}\right) \quad (7)$$

$$\beta = \arctan\left(\frac{v}{\sqrt{u^2 + w^2}}\right) \quad (8)$$

Forces acting on the UAV originate from the gravity force  $F_{grav}$ , propeller force  $F_{prop}$  and aerodynamical  $F_{aero}$  forces. For the sake of clarity, these forces are expressed in the reference frame where they are the simplest. The transformation matrices allow writing them in the desired reference frame.

$$F_{grav}^{R_E} = (0 \ 0 \ g)^T \quad (9)$$

$$F_{prop}^{R_b} = \left( \frac{k}{V} \delta_x \ 0 \ 0 \right)^T [3] \quad (10)$$

$$F_{aero}^{R_a} = \frac{1}{2} \rho S V^2 (-C_x \ C_y \ -C_z)^T \quad (11)$$

where  $g$  is the local acceleration of gravity,  $S$  is the wing surface,  $k$  is a constant,  $\rho$  is the air density, the aerodynamic force coefficients in  $R_a$  are:

$$C_x = C_{x0} + C_{x\alpha}\alpha + C_{x\delta_{ar}}\delta_{ar} + C_{x\delta_{al}}\delta_{al} + C_{x\delta_{er}}\delta_{er} + C_{x\delta_{el}}\delta_{el} + C_{x\delta_{fr}}\delta_{fr} + C_{x\delta_{fl}}\delta_{fl} \quad (12)$$

$$C_y = C_{y\beta}\beta + C_{yp}\frac{bp}{2V} + C_{yr}\frac{br}{2V} + C_{y\delta_r}\delta_r \quad (13)$$

$$C_z = C_{z0} + C_{z\alpha}\alpha + C_{z\delta_{ar}}\delta_{ar} + C_{z\delta_{al}}\delta_{al} + C_{z\delta_{er}}\delta_{er} + C_{z\delta_{el}}\delta_{el} + C_{z\delta_{fr}}\delta_{fr} + C_{z\delta_{fl}}\delta_{fl} \quad (14)$$

Moments acting on the UAV originate from aerodynamical moments:

$$\Gamma_{aero} = \frac{1}{2} \rho S V^2 (bC_l \ \bar{c}C_m \ bC_n) \quad (15)$$

where  $\bar{c}$  is the aerodynamic mean chord and  $b$  is the wing span. The aerodynamic moment coefficients in  $R_b$  are:

$$C_l = C_{l\beta}\beta + C_{lp}\frac{bp}{2V} + C_{lr}\frac{br}{2V} + C_{l\delta_{ar}}\delta_{ar} + C_{l\delta_{al}}\delta_{al} + C_{l\delta_{er}}\delta_{er} + C_{l\delta_{el}}\delta_{el} + C_{l\delta_{fr}}\delta_{fr} + C_{l\delta_{fl}}\delta_{fl} \quad (16)$$

$$C_m = C_{m0} + C_{m\alpha}\alpha + C_{mq}\frac{\bar{c}q}{2V} + C_{m\delta_{ar}}\delta_{ar} + C_{m\delta_{al}}\delta_{al} + C_{m\delta_{er}}\delta_{er} + C_{m\delta_{el}}\delta_{el} + C_{m\delta_{fr}}\delta_{fr} + C_{m\delta_{fl}}\delta_{fl} \quad (17)$$

$$C_n = C_{n\beta}\beta + C_{np}(\alpha)\frac{bp}{2V} + C_{nr}(\alpha)\frac{br}{2V} + C_{n\delta_{ar}}\delta_{ar} + C_{n\delta_{al}}\delta_{al} + C_{n\delta_{er}}\delta_{er} + C_{n\delta_{el}}\delta_{el} + C_{n\delta_{fr}}\delta_{fr} + C_{n\delta_{fl}}\delta_{fl} + C_{n\delta_r}\delta_r \quad (18)$$

It is worth to notice that aerodynamic coefficients depend on each control surface, this writing allows considering

asymmetric faults. These coefficients have been calculated with formulae proposed in [14] where each control surface is considered as a single flap. Due to the smallness of the flight envelope, these coefficients are supposed to be constant for the overall of the flight envelope.

Finally bank angle  $\varphi$  and pitch angle  $\theta$  equations are given by kinematic relations. As it concerns the heading angle and the centre of gravity coordinates, they are not studied here because the FTC problem is an attitude control problem.

The general model of the UAV can be written as:

$$\dot{X} = f(X) + g(X)U \quad (19)$$

In fault-free mode, this aircraft is equipped with two control laws (figure 2), the true airspeed  $V$ , the flight path angle  $\gamma = \theta - \alpha$ <sup>1</sup> and the bank angle  $\varphi$ .

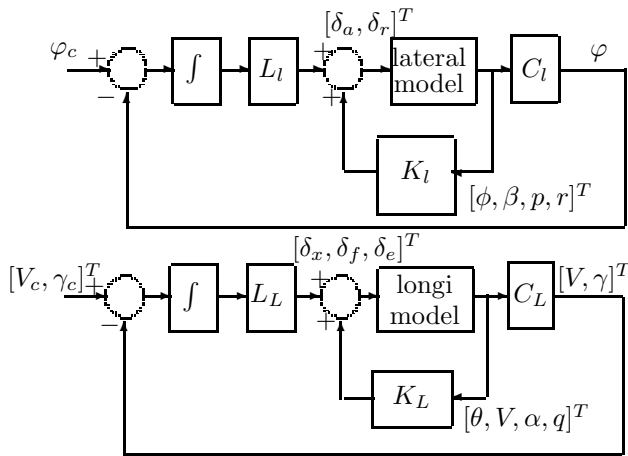


Fig. 2. Lateral and longitudinal control laws in fault-free mode

### III. FAULT TOLERANT STRATEGY

Faults considered are asymmetric stuck control surfaces. When one or several control surfaces are stuck, the equilibrium of forces and moments are broken, the UAV moves away from the fault-free mode operating point and a risk to loose the aircraft exists. A fault tolerant control system may be implemented if and only if a new operating point may be found. When  $k$  control surfaces are stuck, a new operating point exists if the state and control vectors satisfy:

$$0 = f(X_e) + g^h(X_e)U_e^h + g^f(X_e)U_b^f \quad (20)$$

with  $X_e$  the equilibrium state vector,  $U_e^h$  the trim positions of the healthy controls and  $U_b^f$  the faulty control positions. In the following  $e$  and  $e_0$  denote the operating point respectively in faulty mode and the operating point in fault-free mode,  $U^h$  and  $U^f$  denote respectively the healthy and faulty controls.

The FTC strategy proposed consists of three stages. Firstly, a new operating point  $\{X_e, U_e^h\}$  is calculated,

<sup>1</sup>Note that in faulty mode, the longitudinal and lateral axis are coupled and the flight path angle is:  $\gamma = \arcsin(\sin \theta_e \cos \alpha_e \cos \beta_e - \sin \varphi_e \cos \theta_e \sin \beta_e - \cos \varphi_e \cos \theta_e \sin \alpha_e \cos \beta_e)$

UAV non-linearities, state variables limitations and control saturations are taken into account. To compute this new operating point, it is assumed that the faulty control and their positions are known, incidentally a diagnosis system for this UAV was presented in [1]. Furthermore the usual deflection constraints of the healthy control surfaces are released (symmetrical deflections for flaps and elevators, asymmetrical deflections for ailerons) and each one of the  $8 - k$  healthy actuators is controlled separately. Secondly, for this new operating point a linear state feedback controller is designed to ensure a soft transient toward the new equilibrium. Finally, the accommodation is realized by implementing simultaneously the new operating point and the controller.

#### A. Operating point computation in faulty mode

In the sequel, a method is presented to calculate a new operating point. It consists in an optimal reconfiguration of the healthy controls which aims at:

- satisfying equation (20),
- finding solutions included in the state and controls variation ranges,
- keeping the new operating point near the fault-free operating point,
- minimizing the control deflections required to reach the new trims.

Thus the faulty linearized model remains close to the fault-free linearized model and the handling qualities change very little

The healthy controls re-allocation is expressed as an optimization problem with equality and inequality constraints. The cost function  $J$  is:

$$J = \sum_{j=1}^{8-k} r_j (U_j^h - U_{j_{e_0}}^h)^2 + q_V (V - V_{e_0})^2 + q_\alpha (\alpha - \alpha_{e_0})^2 + q_\beta (\beta - \beta_{e_0})^2 \quad (21)$$

where  $r_j$ ,  $q_V$ ,  $q_\alpha$  and  $q_\beta$  are weights. To balance the demands on the healthy actuators, weights  $r_j$  may be adapted to each type of failure.

Under the constraints:

- the stuck control surface position is equal to  $U_b^f$  :
- $$U^f - U_b^f = 0 \quad (22)$$

- the equilibrium conditions:

$$\begin{cases} \dot{\varphi} = 0 \\ \dot{\theta} = 0 \\ \dot{V} = 0 \\ \dot{\alpha} = 0 \\ \dot{\beta} = 0 \\ \dot{p} = 0 \\ \dot{q} = 0 \\ \dot{r} = 0 \end{cases} \quad (23)$$

- the UAV flies level:

$$\begin{cases} \varphi_e = 0 \\ p_e = 0 \\ q_e = 0 \\ r_e = 0 \\ \gamma_e = 0 \end{cases} \quad (24)$$

- state variables and controls are bounded:

$$\begin{cases} X_{min} \leq X \leq X_{max} \\ U_{min}^h \leq U^h \leq U_{max}^h \end{cases} \quad (25)$$

The sequential quadratic programming (SQP) used to solve this problem is CFSQP [11], equations (21) to (25) were programmed in C language and encapsulated in an s-function in order to be used with the Real Time Workshop toolbox of MATLAB. This s-function makes use of the faults characteristics issued from the diagnosis system and returns the operating point in faulty mode  $\{X_e, U_e^h\}$ . This program was tested with an embedded PC (PC104) and returned an operating point in 31ms. For a given failure, when a new operating point exists, it is possible to calculate a linearized model of the UAV,

$$\begin{aligned} \dot{x} &= Ax + Bu^h \\ y &= x \end{aligned} \quad (26)$$

$x$  and  $u^h$  are state and input variations around the operating point  $\{X_e, U_e^h\}$ .

### B. Linear state feedback controller design

After computing the new operating point, a linear state feedback illustrated by figure 3 is calculated. It aims at steering the current state vector toward the new equilibrium. The proportional-integral controllers used in fault-free mode are disconnected during all the accommodation stage because their time constants have destabilizing effects.

In theory one controller has to be designed for each fault situation. An eigenstructure assignment method is used to calculate the controller, it allows setting the UAV modes in the sense of handling qualities. This is done by setting the state and control mode sensitivity. In particular, further to an elevator failure, the throttle reacts abruptly. This effect can be mitigate by decoupling the throttle from the fast modes. The eigenstructure as-

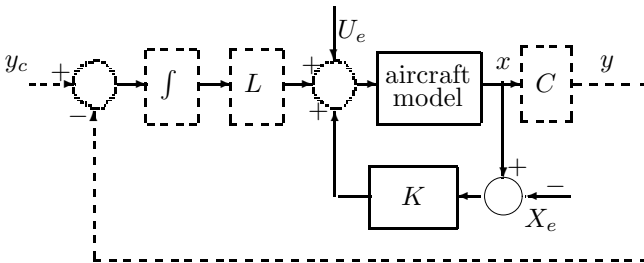


Fig. 3. Control law in faulty mode

signment method is briefly recalled. The state equations (26) and the control laws:

$$u^h = Kx \quad (27)$$

The controller gain  $K$  is calculated in order to place the eigenvalues  $\lambda_i$  of  $A + BK$  and their eigenvectors  $\vec{v}^i$ .

$$(A + BK)\vec{v}^i = \lambda_i \vec{v}^i \quad (28)$$

Let  $K\vec{v}^i = \vec{w}^i$ , then for the  $i^{th}$  eigenvalue  $\lambda_i$ , equation (28) writes:

$$(A - \lambda_i I_d \quad B) \begin{pmatrix} \vec{v}^i \\ \vec{w}^i \end{pmatrix} = \vec{0} \quad (29)$$

The desired eigenvector  $\begin{pmatrix} \vec{v}^i \\ \vec{w}^i \end{pmatrix}$  is spanned by the kernel of the linear map  $(A - \lambda_i I_d \quad B)$ . The  $j^{th}$  row of vector  $\vec{v}^i$  sets the contribution of the eigenvalue  $\lambda_i$  to the state variable  $x_j \in x$ . Just like the  $k^{th}$  row of vector  $\vec{w}^i$  which sets the contribution of the eigenvalue  $\lambda_i$  to the control input  $u_k^h \in u^h$ . For a stuck right elevator  $\delta_{er}$ , tables I and II show the desired eigenvalues and eigenvectors. For each faulty control surface an eigenstructure assignment strategy has to be defined. The duration of this phase is chosen in reference to the slowest time constant of the closed loop.

UAV modes	roll	dutch roll	spiral
poles OL	-13.7	$-0.1 \pm 1.2i$	0.02
poles CL	-14	$-1.5 \pm 1.5i$	-0.5
état	$v^1, v^2$	$v^3$	$v^4, v^5$
$\varphi$	×	×	×
$\theta$	0	0	0
$V$	0	0	0
$\alpha$	0	×	0
$\beta$	×	×	×
$p$	×	×	×
$q$	0	0	0
$r$	×	×	×
	$w^1, w^2$	$w^3$	$w^4, w^5$
$\delta_x$	0	0	0
$\delta_{ar}$	×	×	×
$\delta_{al}$	×	×	×
$\delta_{fr}$	0	0	×
$\delta_{fl}$	0	0	×
$\delta_{el}$	×	×	0
$\delta_r$	0	×	×

TABLE I

UAV MODES IN FAULTY MODE, LATERAL AXIS

UAV modes	short period	phugoid
poles OL	$-6 \pm 6.9i$	$-0.04 \pm 0.4i$
poles CL	$-10 \pm 10i$	$-1 \pm i$
état	$v^6, v^7$	$v^8, v^9$
$\varphi$	0	0
$\theta$	×	×
$V$	×	×
$\alpha$	×	×
$\beta$	0	0
$p$	0	0
$q$	×	×
$r$	0	0
	$w^6, w^7$	$w^8, w^9$
$\delta_x$	0	×
$\delta_{ar}$	×	×
$\delta_{al}$	×	×
$\delta_{fr}$	0	×
$\delta_{fl}$	0	×
$\delta_{el}$	×	0
$\delta_r$	×	0

TABLE II

UAV MODES IN FAULTY MODE, LONGITUDINAL AXIS

### C. Possible improvement

The drawback of this method is that an operating point and a state feedback  $K$  must be calculated for each control surface fault position. However, the SQP algorithm aims at remaining the faulty operating point close to the fault-free. Therefore, for one faulty actuator in various fault positions, the faulty linearized models are little scattered and a single pre-computed robust control may accommodate all the fault positions for this actuator.

## IV. RESULTS

This section reports the design of the the right elevator fault tolerant control system and the simulation results obtained when this control surface is stuck. The computation of the cost function (21) under the constraints (22) to (25) shows that an operating point exists for all the fault positions in the the right elevator deflection range  $[-20^\circ, 20^\circ]$ . Note that rudder failures can not systematically be accommodated because the healthy controls do not supply enough redundant effects.

For each fault position and each operating point, the poles of the linearized model have been plotted on figure 4. These poles are little scattered around their fault free values (red cross) and let to think that a unique controller could accommodate the whole fault positions for this control surface.

As regards the eigenvalue and eigenvector setting, this one is illustrated with table I, it aims at:

- decoupling the longitudinal state variables  $\{\theta, V, \alpha, q\}$  and the lateral state variables  $\{\varphi, \beta, p, r\}$ ,
- decoupling the throttle from the fastest modes in order to control it softly,
- producing a pitch moment with the ailerons. Indeed, when the right elevator jams abruptly, it produces a pitch moment which is mainly balanced with the left elevator. To relieve this control, ailerons are used

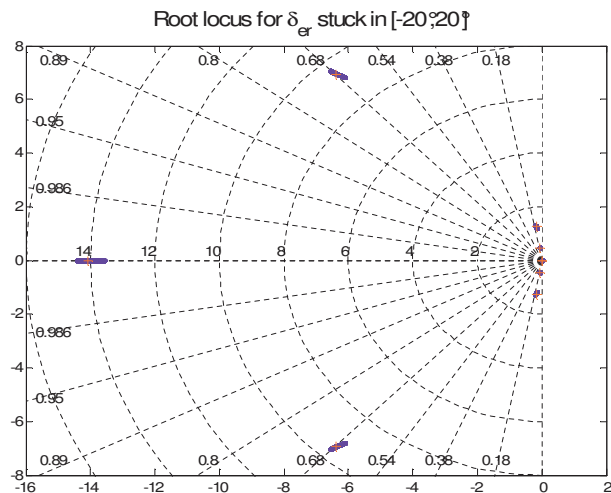
instead of flaps because they have a largest range variation.

- the true airspeed and the flight path angle (slow variables) are controlled with the throttle and the flaps.

In fault free mode, the UAV flies level. At time  $t = 10s$ , the right elevator jams and the faulty position is equal to  $20^\circ$  (figure 5). At time  $t = 10.5s$ , the linear state feedback controller designed for the operating point computed with the CSQP algorithm allows accommodating the fault (blue line) whereas the UAV is lost with the nominal control law (red line). The state variables and the controls are represented on figures (5) to (8).

Figure 7 shows that the two flaps are in their limit stop positions. A recent study [2] has proved that in spite of these saturations, the state vector remained in the null controllable region.

Finally, in the time interval between the fault occurrence time (10s) and the fault accommodation time (10.5s), the UAV is controlled with the nominal controller and the throttle decreases. For this controller, in order to avoid an undesirable shutdown of the motor, the throttle is decoupled from the fastest modes. On the other hand, this strategy allows increasing time for diagnosis and accommodation.

Fig. 4. Root locus,  $\delta_{er}$  stuck on  $[-20^\circ, 20^\circ]$ 

## V. CONCLUSIONS

In this paper, a fault tolerant control strategy was presented for an UAV. In the presence of control surface failures, an optimal re-allocation of the healthy actuators based on a Sequential Quadratic Programming algorithm has been designed and a real time implementation of this algorithm was implemented. In faulty mode, for the new operating point, a linear state feedback controller was designed with an eigenstructure assignment strategy. Present works have already permitted to match this FTC system with a diagnosis system. Future works aim

at estimating the domain of attraction under saturated linear feedback.

REFERENCES

[1] F. Bateman, H. Noura, and M. Ouladsine. An actuator fault detection, isolation and estimation system for an uav using input observers. In *European Control Conference*, Kos, Greece, 2007.  
 [2] F. Bateman, H. Noura, and M. Ouladsine. Null controllability region for an uav with faulty actuators. In *Advanced Control Diagnosis*, Grenoble, France, 2007.  
 [3] J.L. Boiffier. *The dynamics of flight*. Wiley, 1998.  
 [4] R. Brigaud. Working towards a usar stanag. In *Euro UAV*, Paris, France, 2006.

[5] F.W. Burcham, T.A. Maine, C. Gordon Fullerton, and L.D. Webb. Development and flight. Technical Report Technical Paper 3627, NASA, 1996.  
 [6] Collectif. Unmanned aerial vehicle reliability study. Technical report, Office of the Secretary of Defense, 2003.  
 [7] Collectif. Unmanned aerial vehicle road map 2005-2030. Technical report, Office of the Secretary of Defense, 2005.  
 [8] O. Harkegard and S. Torkel Glad. Resolving actuator redundancy-optimal control vs. control allocation. *Automatica*, 44(1):137-144, 2005.  
 [9] D. Ito, J. Georgie, J.Valasek, and D.T. Ward. Reentry vehicle flight control design guidelines: Dynamic inversion. Technical Report NASA/TP-2002-210771, NASA, 2002.  
 [10] J. Jiang and Y. Zhang. Accepting performance degradation in fault-tolerant control system design. *IEEE transactions on control systems technology*, 14:284-292, 2006.  
 [11] Craig Lawrence, Jian L. Zhou, and André L. Tits. User's guide for cfsqp version 2.5: A c code for solving (large scale) constrained nonlinear (minimax) optimization problems, generating iterates satisfying all inequality constraints.  
 [12] M. Napolitano, Y. An, and B. Seanor. A fault tolerant flight control system for sensor and actuator failures using neural network. *Aircraft Design*, 3:103-128, 2000.  
 [13] A.A. Pashilkar, N. Sundararajan, and P. Saratchandran. A fault-tolerant neural aided controller for aircraft auto-landing. *Aerospace Science and Technology*, 10:49-61, 2006.  
 [14] D. P. Raymer. *Aircraft design, a conceptual approach*. AIAA Education series, 1998.  
 [15] S.Thomas, H.G. Kwatny, and B.C. Chang. Nonlinear reconfiguration for asymmetric failures in a six degree-of-freedom f-16. In *American Control Conference*, Boston, USA, 2004.  
 [16] Y.M. Zhang, S. Sivasubramaniam, D. Theillioli, and B. Jiang. Reconfigurable control allocation against partial control effector faults in aircraft. In *International Modeling and Simulation Multiconference*, Buenos Aires, Argentina, 2007.

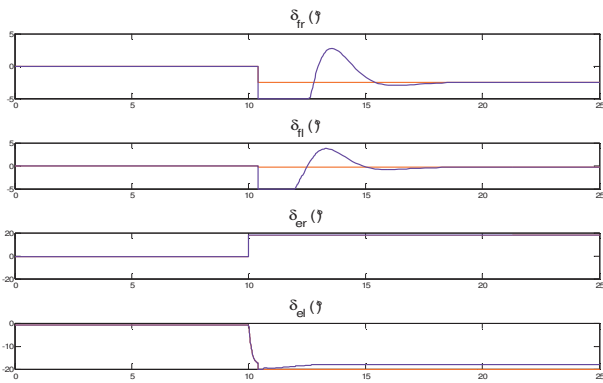


Fig. 5. Right elevator stuck, controls

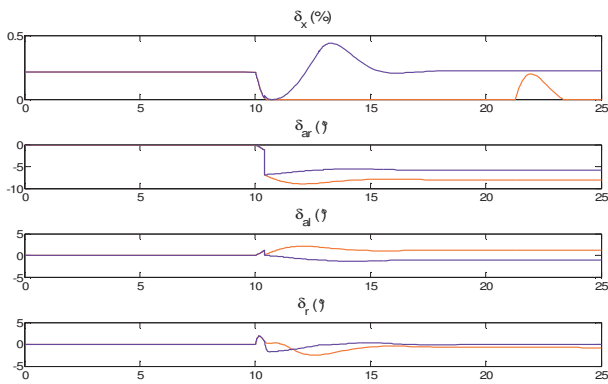


Fig. 6. Right elevator stuck, controls

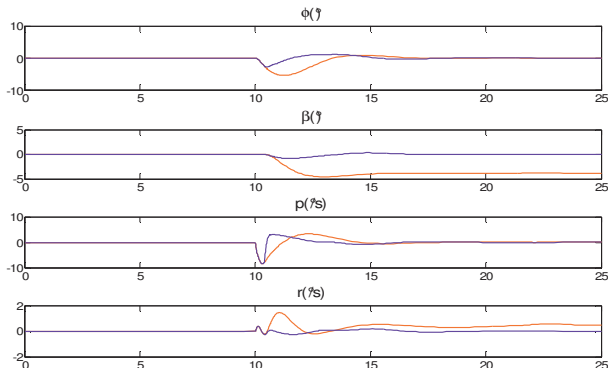


Fig. 7. Right elevator stuck, lateral state variables

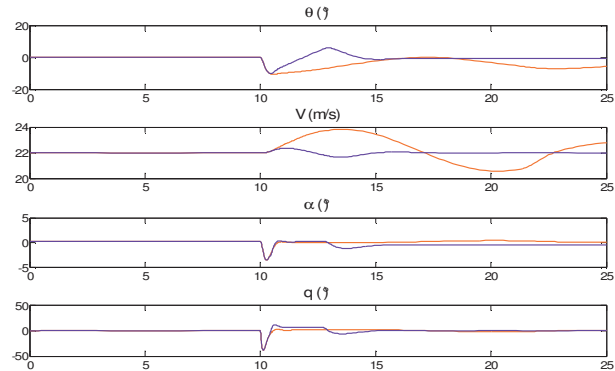


Fig. 8. Right elevator stuck, longitudinal state variables

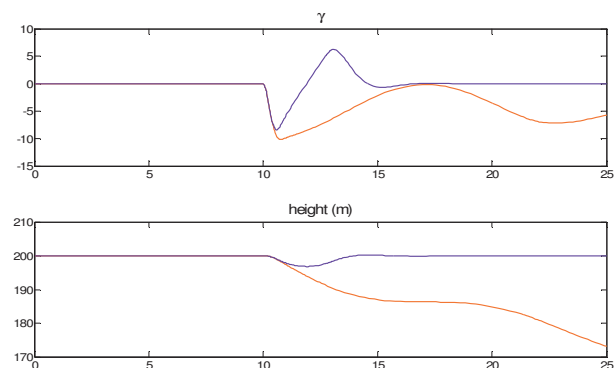


Fig. 9. Right elevator stuck, flight path angle and height